Containerless metal single-crystal growth via electromagnetic levitation

(iD) J. P. Witteveen, M. A. B. Vrielink, R. van Gastel, et al.

View Online   Export Citation   CrossMark

ARTICLES YOU MAY BE INTERESTED IN

A ^{4}He vector zero-field optically pumped magnetometer operated in the Earth-field
Review of Scientific Instruments **92**, 105005 (2021); https://doi.org/10.1063/5.0062791

Design#and implementation of DC-to-DC converter topology for current regulated lightning generator
Review of Scientific Instruments **92**, 104709 (2021); https://doi.org/10.1063/5.0060247

Design#of a tunable turnstile mode converter for high-power microwave applications
Review of Scientific Instruments **92**, 104708 (2021); https://doi.org/10.1063/5.0046613

Containerless metal single-crystal growth via electromagnetic levitation

View Online   Export Citation   CrossMark

J. P. Witteveen,[1,a] 🆔 M. A. B. Vrielink,[1] R. van Gastel,[2] A. van Houselt,[1] and H. J. W. Zandvliet[1] 🆔

AFFILIATIONS

[1]Physics of Interfaces and Nanomaterials, MESA+ Institute for Nanotechnology, University of Twente,
 P.O. Box 217, 7500 AE Enschede, The Netherlands
[2]Surface Preparation Laboratory, Rosbayerweg 159, 1521 RW Wormerveer, The Netherlands

[a]Author to whom correspondence should be addressed: j.p.witteveen@utwente.nl

ABSTRACT

The growth of elemental metal single-crystals is usually achieved through classic growth techniques such as the Czochralski or floating zone methods. Drawbacks of these techniques are the susceptibility to contamination from the crucible and thermal stress-induced defects due to contact with the ambient, which can be mitigated by growing in a containerless environment. We discuss the development of a novel crystal growth apparatus that employs electromagnetic levitation in a vacuum to grow metal single-crystals of superior quality and purity. This apparatus enables two growth modes: containerless undercooled crystallization and levitation-based Czochralski growth. We describe the experimental setup in terms of coil design, sample insertion and collection, seed insertion, and sample position and temperature tracking. As a proof of concept, we show the successful growth of copper single-crystals.

Published under an exclusive license by AIP Publishing. https://doi.org/10.1063/5.0064486

I. INTRODUCTION

Traditionally, the growth of elemental metal single-crystals is achieved through classic growth techniques, such as the Czochralski, Bridgman, or floating zone methods. Using these techniques, decent-quality crystal rods can be fabricated with relative ease for most metals. The rods, typically 10 mm in diameter and lengths up to 100 mm, can be shaped using electrostatic discharge machining and subsequently polished to the desired crystal orientation. For decades, the crystals grown with these methods have been used in a myriad of scientific experiments. As the characterization techniques, such as x-ray standing waves (XSWs), that are used at synchrotron facilities become more and more accurate, the demand for high-quality crystals exceeds the current state-of-the-art quality and purity of metal crystals.

The traditional arsenal of growth methods suffers from a number of drawbacks that hinder the fabrication of perfect single-crystals. First of all, the molten ultrapure source material is in contact with a crucible, typically made of graphite or an oxide material. It is not surprising that this leads to contamination of the metal with impurities coming from the crucible.[1–3] Therefore, extensive research into the crucible material is needed before relatively clean conditions are met.[4]

Second, the crucible creates a thermal gradient within the system, which, in turn, gives rise to crystal defects.[5–7] Although the floating zone method does not directly use a crucible (the rod used as a starting material is, however, usually still shaped in a crucible), this does not mean the material is free from thermal stress. Actually, all growth methods, in one way or another, mechanically suspend the crystalline rod that is in contact with the melt, again leading to thermal stress-induced crystal defects.[8,9]

To overcome these hurdles, it would be useful to grow crystals in a containerless environment. The absence of a crucible solves both the contamination problem and the thermal stress-induced crystal defect problem. This has already been done for very small samples with the use of a drop tube[10] or for larger samples in the microgravity environment of space.[11,12] The drop tube samples are too small for common research applications, and the growth is difficult to control. The crystals grown in space are too expensive from a commercial point of view. The goal is then to be able to grow decent-sized crystals in a containerless environment on the Earth.

In this article, we discuss the development of a novel crystal growth apparatus that employs electromagnetic levitation (EML) in a vacuum to grow elemental metal single-crystals of superior quality and purity. EML relies on the Lorentz force induced by the levitation coil and exerted on the metal sample.[13] A large

high-frequency current is passed through a coil, which generates a large time-varying magnetic field. This alternating field causes an electromotive force (EMF) that leads to eddy currents induced in any conducting sample placed within the coil. These eddy currents are such that the Lorentz force, arising from the currents inside the applied magnetic field, repels the sample away from the coil. During levitation, the gravitational force is balanced by the Lorentz force. In addition to generating a Lorentz force, the eddy currents cause Joule heating of the sample. Through careful coil design, the coupling between levitation and sample temperature can be controlled in order to create a comfortable temperature window suitable for crystal growth.[14]

A few examples exist in the literature based on another form of EML. The levitation-assisted self-seeding crystal growth method makes use of a conventional crucible and an induction heating coil setup, but part of the melt is lifted by the electromagnetic forces to form a seed for the melt still at the bottom of the crucible.[15] Another example is that of a Hukin-type crucible design, where the melt levitates in the crucible, and a single-crystal is grown using the Czochralski technique.[8,16] Still, in both examples, the material is at some point in contact with the crucible, so contamination cannot be completely avoided. Furthermore, the complexity of Hukin crucibles makes it difficult to tailor to multiple masses and materials. In our design, the complete cycle of melting and solidifying the material as a single-crystal is performed while levitating in a truly containerless environment. The classic EML coils that are used are easy to tailor to a wide variety of metals.[13]

It is notoriously difficult to grow defect-free large-sized single-crystals from the platinum group metals, such as iridium, ruthenium, and rhodium. At least equally difficult are the refractory group metals, such as tantalum and tungsten or, in the broader definition of refractory, chromium. Most of these metals share a high melting point well above 2000 K or even above 3000 K in some extreme cases. Metals having such a high melting point are normally very difficult to melt contamination-free, as (water-cooled) crucible material choice becomes even more critical at such high temperatures. The large thermal gradients also make these metals challenging to grow grain-, dislocation-, and defect-free. Although the aim is to keep the apparatus as generic as possible—a slight improvement might also be expected in the crystal growth of lower melting point materials, such as copper—the primary focus lies on the aforementioned metals.

In Sec. II, we first define the design requirements of a fully containerless crystal growth apparatus. Then, we describe the experimental setup in terms of coil design, sample insertion and collection, seed insertion, sample position, and temperature tracking and, more generally, in terms of vacuum considerations, power supply specifications, and required water cooling.

II. METHODS

In order to grow perfect metal crystals, the system should allow the following:

1. The insertion and levitation of a wide variety of metals.
2. Precise control of the sample temperature in both liquid and solid states.
3. The growth of a single-crystal with a well-defined nucleus.

4. The reduction in contamination from parts in contact with the sample as well as from the air.
5. The reduction in thermal gradients in the sample (and seed crystal, if used).
6. Collection of the sample after levitation without inducing crystal defects due to kinetic shocks (i.e., dropping on a solid surface).

A. Coil design and sample temperature control

A classic levitation coil consists of two parts: a bottom coil provides the lift and a smaller upper coil with reversed current polarity stabilizes the sample. Figure 1 shows an example of such a coil. Temperature control is possible since the force, F, is proportional to the magnetic field as $B\nabla B$, whereas the dissipated power, P, in the sample is proportional to $|B|^2$.[13] The temperature follows from the balance of this dissipated power and the radiated power. It is clear that the sample temperature is highest where the magnitude of B reaches its maximum, which is in the middle of the bottom coil. Another "hot zone" is present in the middle of the top coil.

A sample requires a minimum amount of current to levitate, depending on its conductivity. With increasing current, the sample levitates higher in the coil, with asymptotic behavior toward a maximum height between the two coils. The sample temperature approaches the maximum value at the minimum current needed for levitation; since then, the sample is closest to the middle of the bottom coil. It is, however, difficult to achieve stable levitation with this minimum current setting. Upon heating or even melting, the sample conductivity decreases, and a rapid adjustment of the current is required in order to avoid dropping the sample. At high currents, the sample moves toward the second hot zone, where stability is not an issue. Here, the maximum temperature is capped by the maximum current that the power supply can deliver. From a crystal growth point of view, the material properties and coil design determine if it is preferential to melt the sample in the lower or the upper zone. Since the material properties are fixed, careful coil design is of utmost importance, before attempting to grow crystals of a specific metal.

The sample temperature for a given current can be calculated using a simple model,[14] which is based on one of the first analytical descriptions of EML by Fromm and Jehn.[17] This particular model
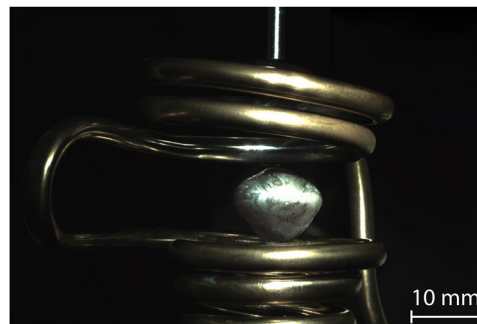

FIG. 1. An aluminum sample levitating in a levitation coil. The bottom coil provides lift, and the top coil stabilizes the sample. A crystal seed is visible above the coil.

improves upon the model by Fromm and Jehn by modeling the coil as a truly 3D path instead of concentric rings and modeling the sample as multiple rings stacked in a spherical geometry instead of a single ring. Where most studies using EML are only interested in measuring certain thermophysical properties,[18] we also want to precisely control the temperature when cooling down in order to crystallize the sample. When a metal sample melts, generally, both the conductivity and the emissivity decrease.[19,20] This causes the temperature of the liquid to increase sharply due to increased Joule heating and decreased thermal radiation. Thus, after melting, nature is not in our favor for subsequent cooling and solidification. Less power input in EML does not necessarily mean a lower temperature due to the sample levitating closer toward the hot zone of the lower coil. Again, the solution is found in careful coil design such that a temperature vs current path exists that enables crossing the melting point in both directions.

Finally, the temperature is proportional to the alternating current frequency as $\sqrt{f}$,[17] which, together with the current magnitude and coil design, makes the frequency the third parameter to vary in finding optimal growth conditions.

Using the model,[14] we can calculate the temperature of a given sample for a given coil and frequency vs the current. The design of the coil is changed manually until a viable solid–liquid–solid cycle is found for a particular material. Parameters to consider are the coil tubing diameter, the distance between the lower and upper coils, the number of windings, and the angle and positions of the windings.[21] For our requirements, described at the beginning of Sec. II, for a generic system with a focus on platinum group and refractory group metals, we manually designed several levitation coils with a 4 mm outer tubing diameter that could levitate, melt, and solidify spherical samples up to 12 mm in diameter for 15 different metals. According to our calculations, this requires frequencies in the order of 100 kHz and currents up to 1000 A. The power source and cooling capabilities of the experimental setup were chosen accordingly.

B. Growth modes

We envision two potential crystal growth modes: containerless undercooled crystallization and levitation-based Czochralski growth.

In the first mode, the sample is levitated and heated until it is completely molten. Then, the current is adjusted such that the liquid cools down to below the melting point. Samples levitated by EML are very stable, and therefore, the formation of a critical nucleus far below the melting temperature might be an issue. A solution is to externally induce the crystallization process using a very thin and sharp needle with a nanoseed at its apex. The temperature should be closely monitored using a pyrometer such that the crystal growth velocity can be controlled, as the quality of the end result greatly depends on this velocity.[22]

In the second mode, the sample is molten but then kept slightly above the melting point. Growth then proceeds as usual with the Czochralski technique, with the difference that the levitation coil, in essence, replaces the crucible. In this case, special attention must be devoted to the design of the top coil, as the magnetic field induced there will also heat the seed crystal. The advantage is that there is less thermal stress between the liquid and the seed. The disadvantage is that the seed might melt if the current becomes too high.

C. Experimental setup

A setup that fulfills the criteria described at the beginning of Sec. II has been designed and constructed. The schematic in Fig. 2 shows a cross section of this experimental setup, and a photograph is shown in Fig. 3. At the heart of the setup is the sample (1), levitated by the water-cooled coil (4). The entire system resides inside a high vacuum chamber (15) to prevent contamination from airborne particles and to prevent oxidation at high temperatures. At the start of an experiment, the sample is held in position in one of the alumina cups of the sample carousel (5). When the current is turned on, the sample starts to levitate. The sample carousel can then be retracted downward using the Z-manipulator (20) and subsequently rotated away from the coil using a rotary feedthrough (23). Note that the manipulator axis (19) is off-center from the middle of the coil/chamber. During levitation, the sample position is tracked with a camera (17). The sample temperature is monitored using a pyrometer (2) so that optimal growth conditions can be obtained by controlling the coil current.

To introduce the seed crystal (3), the seed carousel (6) can be rotated in a position above the coil with the rotary feedthrough (22), which rotates independently from the sample carousel. Since it is possible that the sample might not levitate precisely in the middle of the coil, it is possible to adjust the seed position with the XY-manipulator (21) before lowering the seed to make contact with the molten sample. To avoid large thermal gradients in the hot seed crystal, it is suspended by a tungsten wire (8), which, in turn, is connected to a cold alumina rod (7). The alumina rods of both carousels are in place to electrically decouple all objects in the vicinity of the coil from the chamber, as metallic parts are susceptible to induction heating and could even short circuit the entire system when touching the coil.

After growth, the seed has fused with the crystal so that the crystal can be easily collected through the quick access door (18). If the thin seed crystal cannot support the weight of the sample crystal, the sample will fall when the levitation current is turned off. In this case, the sample falls down on a soft bed of annealed carbon felt (14), after which the surface of the sample can be cleaned and used as usual.

The power source is an Ambrell EKOHEAT system with an output power of 40 kW, capable of delivering a current with a frequency of 50–150 kHz, depending on the capacitor bank (13) configuration. With a typical coil, the maximum current output is in the order of 1500 A.

The camera (17) captures images with 60 frames per second and has a resolution of 3072×2048 pixel^2. In practice, this translates to a resolution where one pixel corresponds to $25 \times 25 \; \mu m^2$, enabling sample tracking with very high accuracy. Figure 1 shows a snapshot of an aluminum sample levitating in a coil. A tracking system relying on in-house developed software tracks the sample position in real-time using either Hough circle detection or blob detection for samples of irregular shape. We have already discussed the dependence of the sample temperature on its height in the coil. Thus, in addition to the pyrometer data, live tracking of the sample position gives valuable information about the temperature, which can be directly applied to optimize the crystal growth.

The above description is, in essence, the heart of the experimental setup. We will now discuss several other characteristics. First of all, the current-carrying rods between the coil and the
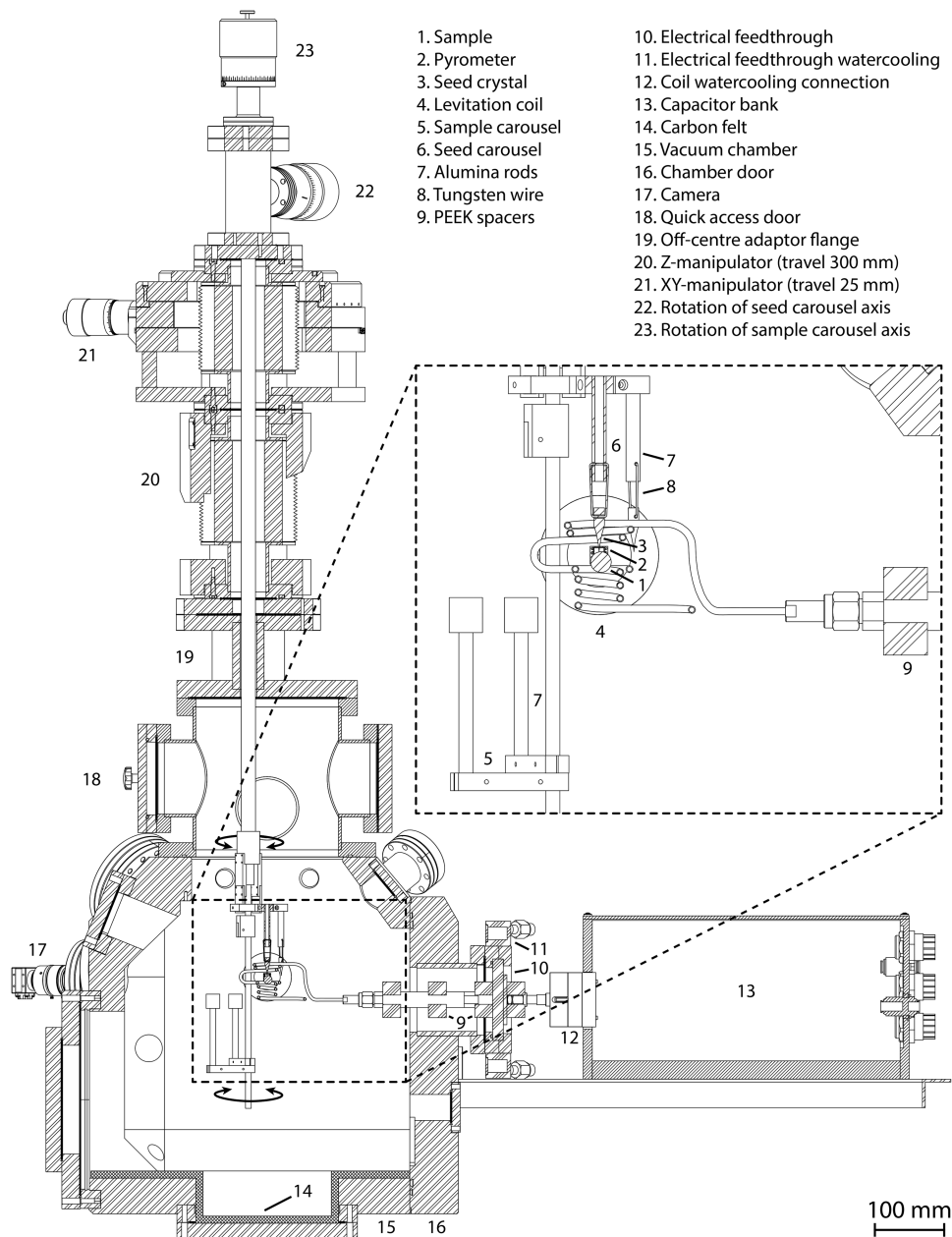
1. Sample
2. Pyrometer
3. Seed crystal
4. Levitation coil
5. Sample carousel
6. Seed carousel
7. Alumina rods
8. Tungsten wire
9. PEEK spacers
10. Electrical feedthrough
11. Electrical feedthrough watercooling
12. Coil watercooling connection
13. Capacitor bank
14. Carbon felt
15. Vacuum chamber
16. Chamber door
17. Camera
18. Quick access door
19. Off-centre adaptor flange
20. Z-manipulator (travel 300 mm)
21. XY-manipulator (travel 25 mm)
22. Rotation of seed carousel axis
23. Rotation of sample carousel axis

100 mm

FIG. 2. Schematic cross section of the experimental setup (drawn to scale).

capacitor bank are subjected to large Lorentz forces due to the opposite current directions and thus tend to separate from each other. Without clamping the rods in place with several polyether ether ketone (PEEK) spacers (9), the maximum deflection at the coil end is in the order of a centimeter. This can potentially put so much force on the electrical feedthrough (10) that it starts leaking or, worse, the ceramic of the feedthrough can break. Even more importantly, without the spacers, the coil itself is greatly deformed since the rods push both endpoints of the coil apart. With these deformations, careful

coil design would not be very useful, as the geometry used in calculations would not match the experimental one. The choice is made for PEEK spacers since a ceramic such as alumina is not able to withstand the forces without fracturing.

Second, the same magnetic fields that levitate and heat the sample also heat the vacuum chamber. Although the coil itself is sufficiently far away from the chamber walls, the electrical feedthrough is heated substantially by the current-carrying rods and thus requires active water cooling (11). In addition, the coil itself needs to be
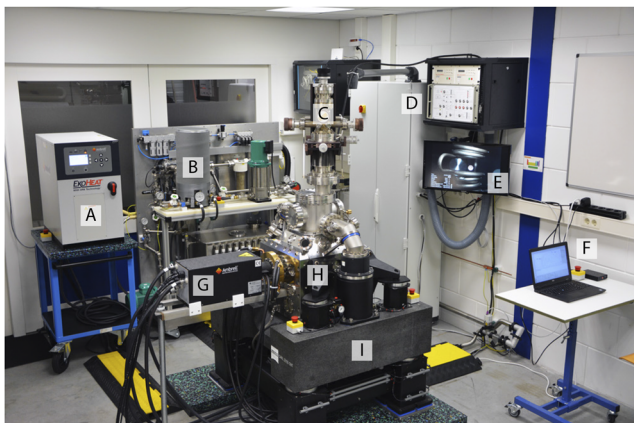
FIG. 3. Photograph of the experimental setup. (a) Power source. (b) Water cooling tank and pump circuit. (c) Vacuum manipulator. (d) Pump and safety control cabinet. (e) Monitor with live camera feed of the coil. (f) Operator workstation. (g) Capacitor bank and electrical feedthrough. (h) Vacuum chamber. (i) Self-leveling table.

FIG. 4. Laue x-ray diffraction image of a copper crystal grown in the levitation setup. The theoretical spot positions are indicated in red together with their corresponding Miller indices. Two unpolished crystals are shown in the inset. The diffraction image is taken at the position of the large green dot visible in the inset.

cooled (12). With an inner coil diameter of 3 mm, 20 bars of water pressure is required to reach a flow of 8 l/min necessary to transport a theoretical maximum power of 40 kW. The coil is attached to a sliding door (16), making it easy to service and replace.

The vacuum chamber can be filled with argon gas to prevent vapor deposition of the hot source material on the viewports. Finally, the entire chamber is placed on a self-leveling granite table to reduce vibrations as much as possible.

III. RESULTS AND DISCUSSION

As a proof of concept, we have grown copper single-crystals in the levitation setup. The experiment was performed by suspending a solid copper rod (diameter of 12.7 mm, 99.99+% purity, Advent R.M.) in a coil. The chamber is pumped down to $5 \cdot 10^{-6}$ mbars, at which point it is filled with 1 bar of argon (99.999% purity, Westfalen). The current in the coil is varied from 175 to 350 A at 93 kHz, which increases the temperature in the rod until the bottom of the rod starts to melt. A liquid droplet is formed, which is levitated in contact with the solid rod. A crystal is subsequently grown by cooling down the sample. The crystal is cooled down by decreasing the current with 4.5 A/min to 70 A, at which point the power is switched off and the crystal is left to cool to room temperature by convection. The experiment was repeated to ensure that the results are reproducible.

Two resulting unpolished copper samples are shown in the inset of Fig. 4. At the position of the large green dot, a Laue x-ray diffraction pattern is recorded, which is also shown in Fig. 4. We can see a clear Cu(111) pattern with no apparent spot smearing or spot splitting, indicating a low defect density. To ensure the monocrystallinity throughout the sample, a series of images has been taken on four locations along the crystal. The locations are spaced 2 mm apart and are indicated by the green dots in Fig. 4. At every position, the Laue diffraction image had a single-crystal appearance as in Fig. 4. A fifth image recorded another 2 mm further showed two distinct
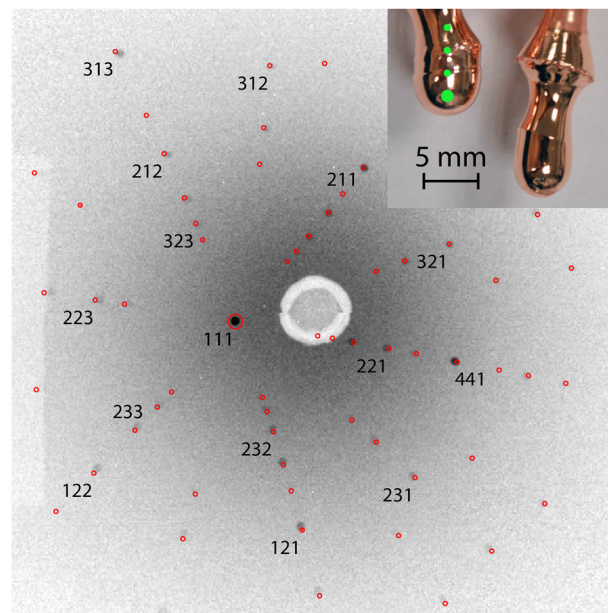
diffraction patterns, indicating a grain boundary. This shows that it is possible to grow levitation-based single-crystals.

To compare the quality of the levitated crystal with a commercially available crystal grown using the traditional Czochralski technique, we aligned and polished both crystals following an identical preparation procedure. The raw diffraction measurements of the crystals are shown in Fig. 5. To the eye, we see no significant differences between the two measurements, indicating that the levitation-based crystal is at least equal in quality to commercially available single-crystals. A more thorough investigation on the quality of the crystal would warrant higher resolution diffraction measurements to
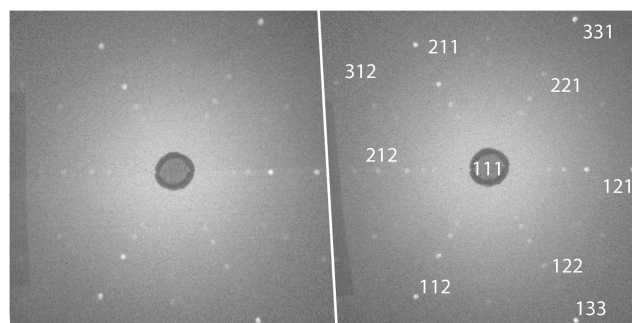

FIG. 5. Raw data of Laue x-ray diffraction image of a copper crystal grown in the levitation setup, aligned and polished (left) compared to a commercially available crystal prepared identically (right). Several spots are labeled with their respective Miller index.
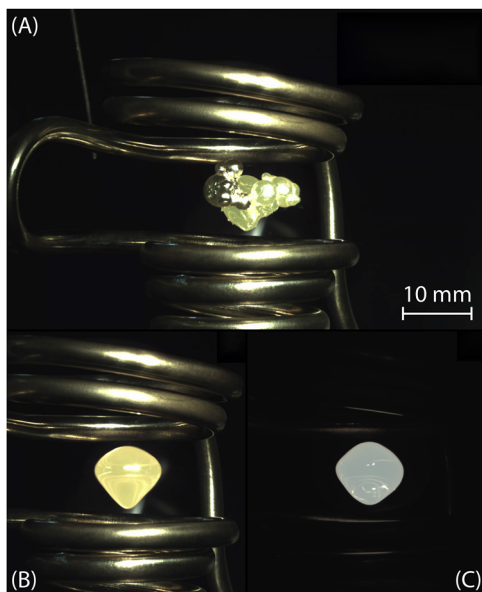
FIG. 6. (a) Multiple copper shots levitating while clumped together. (b) All the copper is molten, and the shape of the liquid droplet is now determined by the surface tension and the magnetic pressure. (c) Low exposure photo of the liquid droplet. The bright white spots are (oxide) contamination that is stirred toward the surface. The reflection of the bottom coil is visible in the droplet as well.

make a quantitative comparison of, for instance, the spot width. In future research, we will also perform contamination measurements to compare our samples with those grown using traditional techniques, where the material is in contact with a crucible, and explore the parameters required for controlled growth of materials with a higher melting point.

Finally, it is important to mention the shape of the samples inserted in the coil. Although spherical samples are easy to model,[13] they can be difficult to acquire commercially for various high purity metals. Moreover, spherical samples have an inherent rotational instability,[23] potentially causing the sample to spin at such high speeds that it fractures. Thus, in practice, it is beneficial to start with an asymmetric sample shape. Very pure metals are often commercially available as shots. In our setup, it is possible to levitate multiple copper shots (99.9999% purity, Goodfellow); see Fig. 6. The magnetic force clumps the individual shots together, while friction prevents the shots from spinning individually. Upon melting, they fuse together to form a single droplet, after which the shape is determined by the interplay of surface tension and magnetic pressure.[24] Thus, it is possible to insert any desired mass of material into the coil while preventing high-speed rotations of the solid object(s). The rotational instability poses less of a problem in the liquid form. On the contrary, the resulting excessive stirring can even be beneficial to purify the sample as (oxide) contamination is separated;[25] see also Fig. 6(c).

IV. CONCLUSION

We presented a novel crystal growth apparatus that employs EML in a vacuum to grow metal single-crystals of superior quality and purity. The system is capable of levitating a wide variety of metals while having precise control over the sample temperature in both the liquid and solid states within 1 K. Crystal growth is possible with either containerless undercooled crystallization or levitation-based Czochralski growth. As a proof of concept, we have shown the growth of copper single-crystals. The crystals grown in the EML setup are at least equal in quality to commercially available single-crystals grown using the traditional Czochralski technique. In future research, we will more accurately determine the crystal quality and compare the purity of crystals grown in our containerless setup with crystals grown in a crucible.

AUTHOR DECLARATIONS

Conflict of Interest

The authors have no conflicts to disclose.

DATA AVAILABILITY

The data that support the findings of this study are available from the corresponding author upon reasonable request.

REFERENCES

[1] M. C. Schubert, J. Schön, F. Schindler, W. Kwapil, A. Abdollahinia, B. Michl, S. Riepe, C. Schmid, M. Schumann, S. Meyer, and W. Warta, "Impact of impurities from crucible and coating on mc-silicon quality—The example of iron and cobalt," IEEE J. Photovoltaics **3**, 1250–1258 (2013).

[2] G. D. Patra, S. G. Singh, D. G. Desai, S. Pitale, M. Ghosh, and S. Sen, "Effect of OH content in the quartz crucible on the growth and quality of CsI single crystals and remedies," J. Cryst. Growth **544**, 125710 (2020).

[3] F. Sturm, M. Trempa, S. Schwanke, K. Schuck, C. Kranert, C. Reimann, and J. Friedrich, "Solid state diffusion of metallic impurities from crucible and coating materials into crystalline silicon ingots for PV application," J. Cryst. Growth **540**, 125636 (2020).

[4] T. B. Reed and R. E. Fahey, "Resistance heated crystal puller for operation at 2000 °C," Rev. Sci. Instrum. **37**, 59–61 (1966).

[5] O. A. Louchev, S. Kumaragurubaran, S. Takekawa, and K. Kitamura, "Thermal stress inhibition in double crucible Czochralski large diameter crystal growth," J. Cryst. Growth **274**, 307–316 (2005).

[6] H. S. Fang, S. Wang, L. Zhou, N. G. Zhou, and M. H. Lin, "Influence of furnace design on the thermal stress during directional solidification of multicrystalline silicon," J. Cryst. Growth **346**, 5–11 (2012).

[7] T. P. Nguyen, Y.-T. Hsieh, J.-C. Chen, C. Hu, and H. B. Nguyen, "Effect of crucible and crystal rotations on the convexity and the thermal stress in large size sapphire crystals during Czochralski growth," J. Cryst. Growth **468**, 514–525 (2017).

[8] J. L. Schmehr and S. D. Wilson, "Active crystal growth techniques for quantum materials," Annu. Rev. Mater. Res. **47**, 153–174 (2017).

[9] M. Plate, A. Krauze, and J. Virbulis, "Three-dimensional modelling of thermal stress in floating zone silicon crystal growth," in *IOP Conference Series: Materials Science and Engineering* (Institute of Physics Publishing, 2018), Vol. 355, p. 012005.

[10] D. Li and D. M. Herlach, "Containerless solidification of germanium by electromagnetic levitation and in a drop-tube," J. Mater. Sci. **32**, 1437–1442 (1997).

[11] J. Yu, N. Koshikawa, Y. Arai, S. Yoda, and H. Saitou, "Containerless solidification of oxide material using an electrostatic levitation furnace in microgravity," J. Cryst. Growth **231**, 568–576 (2001).

[12] S. I. Bakhtiyarov and D. A. Siginer, "Electromagnetic levitation Part III: Thermophysical property measurements in microgravity," Fluid Dyn. Mater. Process. **5**, 1–22 (2009).

[13] E. C. Okress, D. M. Wroughton, G. Comenetz, P. H. Brace, and J. C. R. Kelly, "Electromagnetic levitation of solid and molten metals," J. Appl. Phys. **23**, 545–552 (1952).

[14] J. P. Witteveen, R. van Gastel, A. van Houselt, and H. J. W. Zandvliet "3D modeling of electromagnetic levitation coils," Current Applied Physics (published online, 2021).

[15] Z. Galazka, R. Uecker, and R. Fornari, "A novel crystal growth technique from the melt: Levitation-assisted self-seeding crystal growth method," J. Cryst. Growth **388**, 61–69 (2014).

[16] D. Fort, "An ultrahigh vacuum Czochralski crystal growth system using either hot or cold crucibles," Rev. Sci. Instrum. **64**, 3209–3214 (1993).

[17] E. Fromm and H. Jehn, "Electromagnetic forces and power absorption in levitation melting," Br. J. Appl. Phys. **16**, 653–663 (1965).

[18] L. Gao, Z. Shi, D. Li, G. Zhang, Y. Yang, A. McLean, and K. Chattopadhyay, "Applications of electromagnetic levitation and development of mathematical models: A review of the last 15 years (2000 to 2015)," Metall. Mater. Trans. B **47**, 537–547 (2016).

[19] N. F. Mott, "The resistance of liquid metals," Proc. R. Soc. London, Ser. A **146**, 465–472 (1934).

[20] C. Cagran, C. Brunner, A. Seifter, and G. Pottlacher, "Liquid-phase behaviour of normal spectral emissivity at 684.5 nm of some selected metals," High Temp. High Pressures **34**, 669–679 (2002).

[21] Z. A. Moghimi, M. Halali, and M. Nusheh, "An investigation on the temperature and stability behavior in the levitation melting of nickel," Metall. Mater. Trans. B **37**, 997–1005 (2006).

[22] D. M. Herlach and D. M. Matson, *Solidification of Containerless Undercooled Melts*, 1st ed. (Wiley VCH, 2012).

[23] J. Priede and G. Gerbeth, "Stability analysis of an electromagnetically levitated sphere," J. Appl. Phys. **100**, 054911 (2006).

[24] S. Spitans, E. Baake, B. Nacke, and A. Jakovics, "Numerical modeling of free surface dynamics of melt in an alternate electromagnetic field. Part II: Conventional electromagnetic levitation," Metall. Mater. Trans. B **47**, 522–536 (2016).

[25] G. Wouch, E. C. Okress, R. T. Frost, and D. J. Rutecki, "Electromagnetic levitation facility incorporating electron beam," Rev. Sci. Instrum. **46**, 1122–1123 (1975).